Collision-Induced Anisotropic Relaxation in a Gas Laser

C. H. Wang, W. J. Tomlinson, and R. T. George, Jr.*
Bell Telephone Laboratories, Holmdel, New Jersey 07733
(Received 14 May 1968; revised manuscript received 6 January 1969)

A theory of a single-mode gas laser in a magnetic field has been derived, including the effects of collision-induced anisotropic relaxation. The theory is similar to that obtained by D'yakonov and Perel', but is more general in that it includes anisotropic relaxation, and does not use the Doppler limit to evaluate the third-order integrals. From this theory we have obtained an expression for the critical axial magnetic field strength, and shown that for $j=1 \leftrightarrow j=0$ transitions this expression is particularly simple. Experimental values for the various collision cross sections were obtained by fitting the theoretical expression to the results of a series of measurements of the critical field strength for a He-Ne laser oscillating on the 1.52-μm ($2s_2 \rightarrow 2p_1$, $j=1 \rightarrow j=0$) transition. The cross sections for the relaxation of the electric quadrupole moment of the Ne^{20} $2s_2$ state as a result of collisions with ground-state Ne^{20}, He^3, and He^4 atoms are 5 ± 3, 2.99 ± 0.32 and 2.78 ± 0.37, respectively, in units of 10^{-15} cm^2. The corresponding cross sections for the relaxation of the magnetic dipole moment are a factor of $\frac{5}{3}$ larger. The total radiative lifetime of the Ne $2s_2$ state was found to be 10 nsec, in agreement with other experiments. The experimental cross sections are shown to be in satisfactory agreement with those calculated from the van der Waals collision model.

I. INTRODUCTION

In his well-known laser theory Lamb[1] neglects all collision effects and assumes that the laser action takes place between two nondegenerate levels. This theory has been extended by Sargent, Lamb, and Fork[2] to treat the degeneracies of the levels and the effects of a magnetic field which lifts these degeneracies. It has been found that, with simple phenomenological additions to account for collisions, these theories successfully describe a wide range of experimentally observed phenomena.[3,4] However, it was found that single-cavity-mode, internal-mirror lasers oscillating on $j=1 \rightarrow j=0$ transitions, such as the Ne $2s_2$ - $2p_1$ transition, showed a definite preference for circular polarization (strong coupling of the oppositely circularly polarized components of the mode), while the theory predicted polarization indifference (neutral coupling).[5-7] It was suggested that this effect is a consequence of collision-induced transitions between the magnetic sublevels of the $j=1$ state such that $|\Delta m|=2$ collisions are more probable than $|\Delta m|=1$ collisions.[4,5] Recently it has been shown by Tomlinson and Fork[8] that by including these phenomena in the laser theory in terms of different relaxation rates for the various multipole moments of the $j=1$ state (anisotropic decay) it is possible to obtain quite good agreement between experiment and theory, and hence to obtain a measure of these different relaxation rates.

In general, gas lasers are operated at pressures of the order of 1 Torr, thus only binary collisions need be considered, and because at any one time most of the atoms are in their ground states, the only binary collisions which need be considered are those between an excited atom in one of the laser states and another same or different atom in its ground state. As indicated in the preceding paper,[9] it is useful to divide collision-induced relaxation mechanisms into two categories. In the first category we include collisions in which the initially excited atom does not change its electronic state, although its angular momentum may be reoriented. We will refer to such collisions as m_j - mixing collisions. In the second category we include collisions in which the electronic excitation is transferred from the initially excited atom to the colliding atom. We will refer to these processes as excitation-transfer collisions.

In a laser oscillator intracoherence between the sublevels of each of the laser states is excited by the standing wave optical field in the cavity. (In this section we will use the word "intracoherence" rather loosely to indicate the presence of off-diagonal elements of the density matrix for the Zeeman sublevels of an excited state.) However, since the field is essentially monochromatic it only interacts with atoms having velocities along the laser axis such that their Doppler-shifted transition frequencies fall within a natural linewidth of the cavity frequency. Furthermore the atoms which have interacted with the field are "labeled" because the field also excites an "intercoherence" between the two laser states, and it is this coherence which we measure by means of its interaction with the field. The coherence between the two states cannot be transferred to another atom, so that if an atom which has interacted with the laser field

then transfers its excitation to another atom, it has effectively been removed from the laser. The coherence between the sublevels of one of the states (intracoherence) can be transferred, but since the atom to which the excitation is transferred can have essentially any velocity along the laser axis, the effects of this coherence are diluted by the ratio of the natural width to the Doppler width for the transition, and can usually be neglected. Similarly, radiation trapping also cannot transfer the intercoherence of an active atom, and by the same reasoning as given above we will neglect the intracoherence which is transferred. Therefore, since m_j - mixing collisions and excitation-transfer collisions affect the system in different ways, we can measure separately the relaxation rates of the coherence of the ensemble of atoms with a given velocity component along the laser axis which was initially excited by the laser field, and the rates of excitation transfer and radiative decay.

The situation is somewhat different in a Hanle-effect experiment.[10] In such an experiment the intracoherence in a particular state is excited by absorption of a beam of resonance radiation, and the relaxation rates of the coherence are measured by observing the fluorescence light emitted in some direction by all the atoms in that particular state. There is no way of distinguishing between an atom excited by the exciting beam and an atom excited by an excitation transfer process such as a resonant collision or radiation trapping, since intracoherence is transferred from one atom to another atom of the same kind through the excitation transfer. Therefore in the Hanle effect, one measures the total relaxation rate of the intracoherence of the ensemble of atoms in the excited state but cannot experimentally separate the relaxations by m_j - mixing collisions and by excitation transfers.

In this paper we derive a theory of a single-mode Zeeman laser including the effects of anisotropic relaxation. In particular we obtain an expression for the critical axial magnetic field, which is the magnetic field strength for which the coupling between the circular polarizations is neutral. The critical field is a well-defined experimental quantity, and for $j=1\rightarrow j=0$ transitions the theoretical expression assumes a very simple form. We have made experimental measurements of the critical field strength as a function of gas mixture and pressure for a He-Ne laser oscillating on the 1.52-μm Ne transition ($2s_2\rightarrow 2p_1$, $j=1\rightarrow j=0$). Fitting the theoretical expression to the experimental results we obtain experimental values for cross sections for collision-induced anisotropic relaxation of the Ne^{20} $2s_2$ state as a result of collisions with ground state Ne^{20}, He^3, and He^4 atoms. These cross sections are in satisfactory agreement with those calculated from the van der Waals collision model.[9]

II. FORMULATION OF THE PROBLEM

Because the optical field medium interaction is small compared with the thermal energy (kT), and because the duration of a collision is short compared with the natural lifetime of the atomic states, the collision dynamics can be considered independently of the laser interactions. As a result, at any time t during the laser action an active atom, at position z measured along the axis of the laser with velocity component v along the z axis, can be described by a density operator $\rho(z,v,t)$ with an approximate equation of motion of the form

$$\frac{\partial\rho(z,v,t)}{\partial t}=-i[\mathcal{H}+V(z,t),\rho(z,v,t)]_- -\tfrac{1}{2}[\Gamma,\rho(z,v,t)]_+ +A\rho_1(t)A^+ +\lambda_0(t)+\left(\frac{\partial\rho(z,v,t)}{\partial t}\right)_{\text{col}}. \quad (1)$$

Here $\mathcal{H}$ is the unperturbed Hamiltonian describing the active atom, and $V(z,t)$ is the interaction of the optical field with the atom. The operators Γ and A are included to account for spontaneous decay of the laser states and the feeding of the lower state by the spontaneous decay of the upper laser state respectively. The plus and the minus signs in the subscripts indicate an anticommutator and a commutator respectively. The operator A^+ is Hermitian conjugate to A. With regard to the eigenstates of $\mathcal{H}$, Γ is diagonal and A has no non-zero elements on the diagonal or above it. The λ term represents the pumping excitation, and, finally, the remaining term describes the changes of the density operator by atomic collisions. (Radiation trapping has been neglected for the reasons discussed above although its inclusion here would not complicate the development in this and the following sections.)

It has been shown by D'yakonov and Perel'[11,12] and by Omont[13] that in a representation in terms of irreducible tensor operators the collision, radiative trapping, and spontaneous emission feeding terms are all diagonal, and depend only on the tensor order. We therefore expand the density operator $\rho(z,v,t)$ by

$$\rho(z,v,t)=\sum_{\chi q}\rho_q^{(\chi)}(z,v,t)\,T_{-q}^{(\chi)}, \quad (2)$$

where the reduced density operator $\rho_q^{(\chi)}(z,v,t)$ does not depend on the atomic orientation. The spatial arrangement of the atom is taken into account by the spherical tensor operator $T_{-q}^{(\chi)}$ whose matrix element between the states $|jm\rangle$ and $|j'm'\rangle$ is given by

$$\langle jm|T_{\pm q}^{(\chi)}|j'm'\rangle = (-1)^{j-m\mp q}(2\chi+1)^{1/2}\begin{pmatrix} j & \chi & j' \\ -m & \pm q & m' \end{pmatrix}, \quad (3)$$

and where the quantity in the spherical bracket is the Wigner 3-j symbol.[14]

Taking the matrix elements of Eq. (1) in a coordinate system quantized with respect to the external magnetic field direction and then making the transformation described by Eqs. (2) and (3), one obtains the equation for the reduced density matrix $\rho_q^{(\chi)}(\alpha, \beta, |z, v, t)$ as

$$\begin{aligned}\dot{\rho}_q^{(\chi)}(\alpha,\beta|z,v,t) &= \bar{\lambda}_q^{(\chi)}(\alpha|z,v,t)\delta_{\alpha\beta} \\ &+ \Gamma^{(\chi)}\rho_q^{(\chi)}(\mu,\nu|z,v,t)\,\delta_{\mu a}\delta_{\nu a} \\ &- \gamma_{\alpha\beta}^{(\chi)}\rho_q^{(\chi)}(\alpha,\beta|z,v,t) \\ &- i[\omega_{\alpha\beta}-q\Omega]\rho_q^{(\chi)}(\alpha,\beta|z,v,t) \\ &+ [\text{field-medium interaction}], \end{aligned} \quad (4)$$

where in the notation for ρ, α (or β) index either the upper level a or the lower level b, and μ and ν index the levels with parity opposite to that of α and β, respectively. (For example, if $\alpha = a$, then $\mu = b$, etc.)

The first term on the right-hand side of Eq. (4) is the external pumping excitation, and assuming isotropic pumping $\bar{\lambda}_q^{(\chi)}(\alpha|z,v,t)$ is given by

$$\bar{\lambda}_q^{(\chi)}(\alpha|z,v,t) = \lambda_\alpha(z,v,t)(2j_\alpha+1)^{1/2}\delta_{\chi 0}\delta_{q0}, \quad (5)$$

where $\lambda_\alpha(z,v,t)$ is the rate of excitation of atoms into state α at position z, with velocity v, at time t.

The second term describes isotropic as well as anisotropic pumping of the lower level by the spontaneous decay of the upper level, and $\Gamma^{(\chi)}$ is given by

$$\Gamma^{(\chi)} = \gamma(2j_a+1)(-1)^{j_a+j_b+\chi+1}\begin{Bmatrix} j_a & j_a & \chi \\ j_b & j_b & 1 \end{Bmatrix}, \quad (6)$$

where γ is the reciprocal lifetime for the spontaneous transition between the laser states.

The quantity $\gamma_{\alpha\beta}^{(\chi)}$ in the third term is given by

$$\gamma_{\alpha\alpha}^{(\chi)} \equiv \gamma_\alpha^{(\chi)} = \gamma_\alpha + (\gamma_\alpha^{(\chi)})_{\text{col}}, \quad (7)$$

$$\gamma_{ab}^{(\chi)} = \gamma_{ba}^{(\chi)} = \tfrac{1}{2}(\gamma_a+\gamma_b) + (\gamma_{ab}^{(\chi)})_{\text{col}}. \quad (8)$$

Here γ_α is the rate of spontaneous decay of atoms from state α to all other states. Collision-induced relaxations are represented by $(\gamma_\alpha^{(\chi)})_{\text{col}}$ and $(\gamma_{ab}^{(\chi)})_{\text{col}}$. From the discussion above, it should be clear that since m_j-mixing collisions do not remove the atom from the ensemble of atoms interacting with the laser field they cannot contribute to $(\gamma_\alpha^{(0)})_{\text{col}}$. On the other hand, collisions in which the excitation is transferred will contribute equally to all the $(\gamma_\alpha^{(\chi)})_{\text{col}}$. Therefore $\gamma_\alpha^{(0)}$ is the sum of the spontaneous decay rate and the rates of excitation transferring collisions, while the quantities $\gamma_\alpha^{(\chi)} - \gamma_\alpha^{(0)}$ for $\chi > 0$ describe the effects of m_j-mixing collisions. The quantity $(\gamma_{ab}^{(\chi)})_{\text{col}}$ represents the collision-induced relaxation of the coherence between the two laser states, and for electric dipole radiation only the case $\chi = 1$ is important. For simplicity we shall write γ_{ab} for $\gamma_{ab}^{(1)}$.

The fourth term of Eq. (4) describes the motion of the free atom in the magnetic field; $\omega_{\alpha\beta}$ is the transition frequency of the free atom in the absence of the magnetic field, and $\Omega = gH\mu_B$, where g is the g factor, μ_B is the Bohr magneton, and H is the external magnetic field. To derive this term we assume that the g factors of the upper and the lower levels are the same. This assumption is justified provided

$$(g_a - g_b) \ll \gamma_\alpha^{(\chi)}/\mu_B H$$

and of course is always valid if one of the states has $j = 0$.

Finally, the field-medium interaction term of Eq. (4) is given by

$$\begin{aligned}[\text{field-medium interaction}] &= i(-1)^{q+j_a+j_\beta} \\ &\sum_{\chi' q'}\sum_M E_{-M}(z,t)[(2\chi+1)(2\chi'+1)]^{1/2} \\ &\times \begin{pmatrix} 1 & \chi' & \chi \\ -M & q' & -q \end{pmatrix}\Bigg[p(\alpha,\mu)\rho_q^{(\chi')}(\mu,\beta|z,v,t) \\ &\times \begin{Bmatrix} 1 & \chi' & \chi \\ j_\beta & j_\alpha & j_\mu \end{Bmatrix} + (-1)^{\chi+\chi'} \\ &\times \rho_q^{(\chi')}(\alpha,\nu|z,v,t)p(\nu,\beta)\begin{Bmatrix} 1 & \chi' & \chi \\ j_\alpha & j_\beta & j_\nu \end{Bmatrix}\Bigg], \end{aligned} \quad (9)$$

where $p(\alpha, \mu)$ is the reduced electric dipole matrix element between the levels α and μ, defined according to the convention used by Edmonds.[14] The

quantities in curvy brackets are Wigner 6-j symbols.[14] $E_M(z,t)$ is the Mth circular component of the field given by

$$E_M(z,t)=\hat{\epsilon}_M\cdot\vec{E}(z,t)$$

and $$\vec{E}(z,t)=\{\vec{\mathcal{E}}(t)e^{i\omega t}+\vec{\mathcal{E}}^*(t)e^{-i\omega t}\}\sin kz\,, \quad (10)$$

where $\hat{\epsilon}_M$ is the unit vector in the spherical tensor basis, and k is the reciprocal wavelength of the transition. We have neglected any circular birefringence in the cavity, or the presence of more than one spatial mode of the cavity as these are unimportant for the experimental situations we consider. In the next section we solve Eq. (4) to obtain expressions for the amplitude and polarization of the laser field.

III. LASER THEORY

In this section we derive theoretical expressions describing the laser field by means of the technique developed by Lamb.[1] We solve Eq. (4) by iteration to obtain an expression for the macroscopic polarization induced in the laser medium by the optical field. This expression is then substituted into Maxwell's equations to obtain a set of expressions for the amplitudes and frequencies of the polarization components of the field.

The qth circular component of the polarization induced in the medium by the field can be written as

$$\langle P_q(z,t)\rangle=\{\langle P_q(t)\rangle e^{i\omega t}+\langle P_q^*(t)\rangle e^{-i\omega t}\}\sin kz. \quad (11)$$

The positive frequency part is related to the reduced density matrix $\rho_q^{(1)}(a,b\,|z,v,t)$ by

$$\langle P_q^*(t)\rangle e^{-i\omega t}=(-1)^{\Delta j}3^{-1/2}\int_{-\infty}^{\infty}dv f(v)p(a,b)\rho_q^{(1)}(b,a,|z,v,t), \quad (12)$$

where $f(v)$ is the velocity distribution of the active atom. Iterating Eq. (4), in the rotating wave approximation, to the third order in the electric field amplitudes, we can write the result for $\langle P_q^*(t)\rangle$ in the form

$$\langle P_q^*(t)\rangle=\langle P_q^*(t)\rangle^{(1)}+\langle P_q^*(t)\rangle^{(3)}. \quad (13)$$

The first order or linear polarization is given by

$$\langle P_q^*(t)\rangle^{(1)}=-(-1)^{\Delta j}\tfrac{1}{3}N(t)(p^2/ku)Z(\Gamma_1)\mathcal{E}_q^*(t), \quad (14)$$

where $N(t)$ is the excitation density given by

$$N(t)=\frac{\lambda_a(t)}{\gamma_a^{(0)}}-\frac{\lambda_b(t)}{\gamma_b^{(0)}}\left\{1+\frac{\Gamma^{(0)}}{\lambda_b(t)}\frac{\lambda_a(t)}{\gamma_a^{(0)}}\right\}, \quad (15)$$

where u is the mean velocity of the atoms. The function $Z(\Gamma)$ is the plasma-dispersion function[1] defined as

$$Z(\Gamma)=iku\int_0^{\infty}d\tau\exp\{-\Gamma\tau-\tfrac{1}{4}k^2u^2\tau^2\}, \quad (16)$$

and the quality Γ_1 is given in Eq. (21). The third-order term in the nonlinear polarization is given by

$$\langle P_q^*(t)\rangle^{(3)}=-\frac{(-1)^{\Delta j}N(t)}{4}\frac{p^4}{ku}\sum_{\chi'q'}\sum_{ll'q''}(-1)^{q+q'}(2\chi'+1)\begin{pmatrix}1&\chi'&1\\ l&-q'&q\end{pmatrix}\begin{pmatrix}1&1&\chi'\\ -l'&q''&-q'\end{pmatrix}$$

$$\times[\vec{Y}(\chi')\cdot\vec{W}(\chi'|qq'q''l')]\,\mathcal{E}_{-l}^*(t)\,\mathcal{E}_{-l'}(t)\,\mathcal{E}_{q''}^*(t), \quad (17)$$

where the $\vec{Y}(\chi')$ vector is given by

$$\vec{Y}(\chi')=\left[\begin{Bmatrix}1&\chi'&1\\ j_b&j_a&j_b\end{Bmatrix}^2,\ \begin{Bmatrix}1&\chi'&1\\ j_b&j_a&j_b\end{Bmatrix}\begin{Bmatrix}1&\chi'&1\\ j_a&j_b&j_a\end{Bmatrix},\ \begin{Bmatrix}1&\chi'&1\\ j_a&j_b&j_a\end{Bmatrix}^2\right]$$

$$\equiv[\,Y_1(\chi'),Y_2(\chi'),Y_3(\chi')]\ . \tag{18}$$

The $\vec{W}(\chi'|qq'q''l')$ vector is given by

$$\vec{W}(\chi'|qq'q''l')\equiv[\,W_1,W_2,W_3]\ , \tag{19}$$

where

$$W_1=\left\{\frac{1}{\Gamma_2}\left(\frac{Z(\Gamma_1)-Z(\Gamma_3)}{\Gamma_3-\Gamma_1}+\frac{Z(\Gamma_1)+Z(\Gamma_3)}{\Gamma_1+\Gamma_3}\right)+\frac{1}{2(\Gamma_1-\Gamma_3)}\left(\frac{Z(\Gamma_1)-Z(\tfrac{1}{2}\Gamma_2)}{\Gamma_1-\tfrac{1}{2}\Gamma_2}-\frac{Z(\Gamma_3)-Z(\tfrac{1}{2}\Gamma_2)}{\Gamma_3-\tfrac{1}{2}\Gamma_2}\right)\right\}$$

$$+\left\{\frac{1}{\Gamma_2}\left(\frac{Z(\Gamma_1)-Z(\Gamma_3')}{\Gamma_3'-\Gamma_1}+\frac{Z(\Gamma_3')+Z(\Gamma_1)}{\Gamma_3'+\Gamma_1}\right)+\frac{1}{2(\Gamma_1-\Gamma_3')}\left(\frac{Z(\Gamma_1)-Z(\tfrac{1}{2}\Gamma_2)}{\Gamma_1-\tfrac{1}{2}\Gamma_2}-\frac{Z(\Gamma_3')-Z(\tfrac{1}{2}\Gamma_2)}{\Gamma_3'-\tfrac{1}{2}\Gamma_2}\right)\right\},$$

$$W_2=-(-1)^{\chi'}\Gamma(\chi')\left\{\frac{1}{\Gamma_2\Gamma_2'}\left(\frac{Z(\Gamma_1)-Z(\Gamma_3)}{\Gamma_3-\Gamma_1}+\frac{Z(\Gamma_1)+Z(\Gamma_3)}{\Gamma_1+\Gamma_3}\right)+\frac{1}{(\Gamma_2'-\Gamma_2)(\Gamma_1-\Gamma_3)}\left(\frac{Z(\Gamma_1)-Z(\tfrac{1}{2}\Gamma_2)}{\Gamma_1-\tfrac{1}{2}\Gamma_2}\right.\right.$$

$$\left.-\frac{Z(\Gamma_3)-Z(\tfrac{1}{2}\Gamma_2)}{\Gamma_3-\tfrac{1}{2}\Gamma_2}\right)+\frac{1}{\Gamma_2\Gamma_2'}\left(\frac{Z(\Gamma_1)-Z(\Gamma_3')}{\Gamma_3'-\Gamma_1}+\frac{Z(\Gamma_1)+Z(\Gamma_3')}{\Gamma_3'+\Gamma_1}\right)+\frac{1}{(\Gamma_2'-\Gamma_2)(\Gamma_1-\Gamma_3')}$$

$$\left.\times\left(\frac{Z(\Gamma_1)-Z(\tfrac{1}{2}\Gamma_2)}{\Gamma_1-\tfrac{1}{2}\Gamma_2}-\frac{Z(\Gamma_3')-Z(\tfrac{1}{2}\Gamma_2)}{\Gamma_3'-\tfrac{1}{2}\Gamma_2}\right)\right\}\ ,$$

$$W_3=\text{same as } W_1 \text{ with } \Gamma_2 \text{ replaced by } \Gamma_2' \tag{20}$$

and $\Gamma_1=\gamma_{ab}+i(\omega_{ab}-\omega)-iq\Omega$, $\Gamma_2=\gamma_b^{(\chi')}-iq'\Omega$, $\Gamma_2'=\gamma_a^{(\chi')}-iq'\Omega$,

$$\Gamma_3=\gamma_{ab}+i(\omega_{ab}-\omega)-iq''\Omega\ ,\quad \Gamma_3'=\gamma_{ab}+i(\omega-\omega_{ab})+il'\Omega\ . \tag{21}$$

Equation (17) is a generalization of D'yakonov and Perel's result[12] and, in the Doppler limit ($ku\gg\gamma_{ab}$), can be readily reduced to Eq. (13) of Ref. 12 if the superscript χ' is removed from the decay rates in Eq. (21).

For the case of a magnetic field oriented along the laser axis, Eq. (17) reduces to

$$\langle P_{\pm1}^*\rangle^{(3)}=-(-1)^{\Delta j}N(t)\tfrac{1}{4}(p^4/ku)\sum_{\chi'}(2\chi'+1)$$

$$\times\left[\begin{pmatrix}1&\chi'&1\\-1&0&1\end{pmatrix}^2\vec{Y}(\chi')\cdot\vec{W}(\chi'|\pm1,0,\mp1,\mp1)\,\mathcal{E}_{\pm1}^*|\mathcal{E}_{\pm1}|^2\right.$$

$$+\left\{(-1)^{\chi'}\begin{pmatrix}1&\chi'&1\\-1&0&1\end{pmatrix}^2\vec{Y}(\chi')\cdot\vec{W}(\chi'|\pm1,0,\pm1,\pm1)\right.$$

$$\left.\left.+\begin{pmatrix}1&\chi'&1\\1&-2&1\end{pmatrix}^2\vec{Y}(\chi')\cdot\vec{W}(\chi'|\pm1,\pm2,\pm1,\mp1)\right\}|\mathcal{E}_{\mp}|^2\mathcal{E}_{\pm1}^*\right]\ . \tag{22}$$

From this expression for the dipole moment we can easily extract the expressions for the coefficients in the amplitude and frequency determining equations.[2,12] Dropping scale factors the self- and cross-saturation coefficients of the axial magnetic field case are given by

$$\beta_{\pm}=\mathrm{Im}\sum_{\chi'}(2\chi'+1)\begin{pmatrix}1&\chi'&1\\-1&0&1\end{pmatrix}^2\vec{Y}(\chi')\cdot\vec{W}(\chi'|\pm1,0,\mp1,\mp1) \tag{23}$$

and

$$\theta_{\pm\mp} = \mathrm{Im}\sum_{\chi'} (2\chi'+1)\left\{(-1)^{\chi'}\begin{pmatrix}1 & \chi' & 1\\ -1 & 0 & 1\end{pmatrix}^2 \vec{Y}(\chi')\cdot\vec{W}(\chi'|\pm 1,0,\pm 1,\pm 1)\right.$$

$$\left. +\begin{pmatrix}1 & \chi' & 1\\ 1 & -2 & 1\end{pmatrix}^2 \vec{Y}(\chi')\cdot\vec{W}(\chi'|\pm 1,\pm 2,\pm 1,\mp 1)\right\}, \tag{24}$$

respectively. Here Im indicates the imaginary part.

For an isotropic-cavity, single-cavity-mode laser in an axial magnetic field with the cavity frequency tuned to the atomic line center, there are only two possible solutions for the intensities of the two oppositely circularly polarized components of the electric field in the laser. If the product of the self-saturation coefficients of the two polarization components of the field ($\beta_+\beta_-$) is greater than the product of their cross-saturation coefficients ($\theta_{+-}\theta_{-+}$), the laser will oscillate on both polarizations simultaneously with equal amplitudes (but possibly different frequencies). If $\beta_+\beta_-$ is less than $\theta_{+-}\theta_{-+}$ the laser will oscillate in either circular polarization, but in only one at a time. When ($\beta_+\beta_- - \theta_{+-}\theta_{-+}$) passes through zero the laser will switch between these two modes of operation, so that the condition $\beta_+\beta_- = \theta_{+-}\theta_{-+}$ gives us an equation for the critical axial magnetic field strength, H_c, at which this switch will occur. Substituting the expressions for the betas and thetas in the above equation and taking the Doppler limit, we obtain the result

$$\left(\frac{Y_3(1)}{\gamma_a^{(1)}} + \frac{Y_1(1)}{\gamma_b^{(1)}} - \frac{Y_2(1)\Gamma(1)}{\gamma_a^{(1)}\gamma_b^{(1)}}\right)\left(1+\frac{\gamma_{ab}^2}{\gamma_{ab}^2+\Omega_c^2}\right) = \left(\frac{2\gamma_{ab}^2}{\gamma_{ab}^2+\Omega_c^2}\right)\left(Y_3(2)\frac{\gamma_a^{(2)} - 2\Omega_c^2/\gamma_{ab}}{(\gamma_a^{(2)})^2+4\Omega_c^2}\right.$$

$$\left. + Y_1(2)\frac{\gamma_b^{(2)} - 2\Omega_c^2/\gamma_{ab}}{(\gamma_b^{(2)})^2+4\Omega_c^2} - Y_2(2)\Gamma^{(2)}\frac{\gamma_a^{(2)}\gamma_b^{(2)} - 2\Omega_c^2[(\gamma_a^{(2)}+\gamma_b^{(2)})/\gamma_{ab}+2]}{[(\gamma_a^{(2)})^2+4\Omega_c^2][(\gamma_b^{(2)})^2+4\Omega_c^2]}\right), \tag{25}$$

where $\Omega_c = \mu_B g H_c$.

Equation (25) is a cubic equation in Ω_c^2, but only the positive real solution, if any, represents a physically realizable magnetic field. It can be shown that for reasonable values of the gammas for transitions of the type $j \longleftrightarrow j+1$ with $j \geq \frac{1}{2}$, or $j=\frac{1}{2} \longleftrightarrow j=\frac{1}{2}$ there are no such solutions so that lasers oscillating on these transitions always oscillate in both circular polarizations (under the specified conditions). On the other hand, for transitions of the type $j \longleftrightarrow j$ with $j \geq 1$ or $j=1 \longleftrightarrow j=0$ there is always one and only one such solution. As is described in the next section the critical field is a well-defined experimental quantity which can be measured with considerable precision. In general it is a function of the six variables $\gamma_a^{(1)}$, $\gamma_a^{(2)}$, $\gamma_b^{(1)}$, $\gamma_b^{(2)}$, γ_{ab}, and γ, but there is one case for which the situation is considerably simpler. For a $j=1 \longleftrightarrow j=0$ transition, $Y_3(1)=Y_3(2)=-\frac{1}{9}$, and $Y_2(1)=Y_2(2)=Y_1(1)=Y_1(2)=0$. Substituting these values into Eq. (25) we find that the resulting equation is only a quadratic in Ω_c^2, and it is simply a matter of a little algebra to show that

$$H_c = (\mu_B g)^{-1}[-b+(b^2+c)^{1/2}]^{1/2}, \tag{26}$$

where $b = \gamma_{ab}^2 + \frac{1}{2}\gamma_a^{(1)}\gamma_{ab} + \frac{1}{8}(\gamma_a^{(2)})^2$, (27)

$$c = \tfrac{1}{2}\gamma_a^{(2)}\gamma_{ab}^2(\gamma_a^{(1)} - \gamma_a^{(2)}). \tag{28}$$

Note that in this case H_c depends only on $\gamma_a^{(1)}$, $\gamma_a^{(2)}$, and γ_{ab}, and is independent of the spontaneous transition rate. [We have assumed $j_a=1$, $j_b=0$, but for the case $j_a=0$, $j_b=1$ one need only interchange the subscripts a and b in Eqs. (27) and (28).] In the limiting case $\gamma_a^{(1)} = \gamma_a^{(2)}$ it is easy to see that $H_c=0$ as predicted by the theories which neglect anisotropic relaxation.

IV. EXPERIMENTAL TECHNIQUES AND PROCEDURES

For axial magnetic fields greater than the critical field strength, and small detuning, a laser oscillating on a $j = 1$ to $j = 0$ transition will oscillate simultaneously on the two oppositely circularly polarized components of the cavity mode. The intensities of these two components show a rather sharp crossover as the cavity is tuned through line center. For sufficiently small detuning the difference of the intensities of the two polarizations is a linear function of detuning with a zero at line center and a slope inversely proportional to the amount by which the magnetic field exceeds the critical field. (This phenomenon is discussed at some length in Refs. 4 and 15.) This characteristic of a $j = 1$ to $j = 0$ laser can be used as a frequency discriminator for a control system to stabilize the frequency of the laser,[15] and it also provides us with a convenient method to determine the critical field strength. If we measure the slope of the curve of intensity difference as a function of detuning for various magnetic field strengths, and plot the reciprocal of the slope versus magnetic field, we obtain a straight line which intercepts the magnetic field axis at the critical field strength.

The relative slope can be measured by modulating the length of the cavity and measuring the amplitude of the modulation of the intensity difference. The only problem is that as we approach the critical field the width of the intensity crossover region approaches zero so that we must use a low-amplitude modulating signal and keep the laser tuned to the line center to within about a part in 10^8. The method for accomplishing this in illustrated in Fig. 1. The beam from the laser passes through a $\lambda/4$ plate which converts the two circular polarizations into orthogonal linear polarizations. The yttrium-iron-garnet modulator

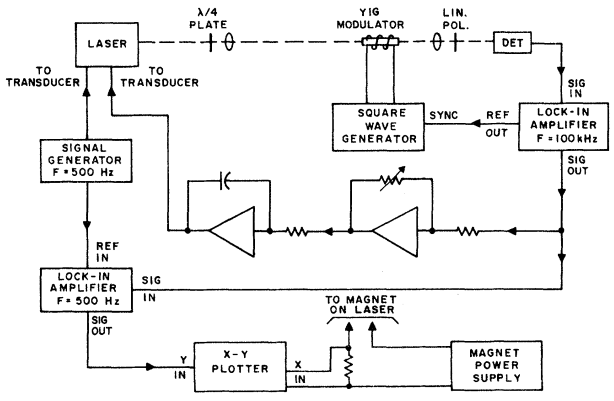

FIG. 1. Block diagram of the experimental arrangement.

rotates the planes of polarizations $\pm 45°$ so that they are alternately parallel or antiparallel to the axis of the linear polarizer. In this way the $\lambda/4$ plate, the modulator, and the polarizer act as an optical polarization chopper alternately passing the two circular polarizations to the detector. This signal is then demodulated in a lock-in synchronous amplifier to produce an output signal proportional to the difference of the intensities of the two opposite circular polarizations. The lock-in is operated at a carrier frequency of about 100 kHz to provide a difference signal with a bandwidth of the order of 10 kHz. The difference signal is amplified and integrated to provide a correction signal to keep the laser tuned to line center. This control loop is identical to that described in Ref. 15 as the slow loop and the reader is referred to that paper for further details on the control system. The signal generator shown on the left side of Fig. 1 drives an electrostrictive transducer to modulate the cavity length at a frequency of about 500 Hz. The gain of the control loop is kept sufficiently low that it has negligible response at this frequency, thus the intensity difference signal from the lock-in amplifier will contain a signal at 500 Hz with an amplitude proportional to the slope of the curve of intensity difference versus detuning. This signal is then demodulated in a second lock-in amplifier to obtain a signal proportional to the slope. An X-Y plotter records this signal as a function of magnetic field. The 500-Hz modulation frequency was picked to be above the response of the control loop, but below the frequency at which the laser-medium response-time effects (described in Ref. 15) become appreciable. The amplitude of the modulation is chosen to produce a frequency modulation less than the width of the linear slope region at the lowest magnetic field at which data are recorded.

The laser was the same as was used for the experiments described in Ref. 15. It is an internal mirror laser with a mirror spacing of 26 cm and a 20 cm long × 2-mm diameter capillary discharge. The laser was connected to a gas-handling system so that gas pressures and mixtures were readily adjustable. Only isotopically pure gases were used (99.99% Ne^{20}, 99.97% He^3, 99.99% He^4). The gas pressures were measured with an MKS Baratron model 90 capacitance manometer for which the manufacturer's calibration indicates an absolute accuracy of better than 0.05 Torr in the pressure region covered by the present experiments. The magnetic field coil was wound directly on the capillary discharge tube thus it was not possible to measure the magnetic field directly. However, at the same time as the coil was wound, an "identical" coil was wound on a tube with the same outside diameter as the capillary but an inside diameter sufficient to admit a Gaussmeter probe. Cali-

brating the Gaussmeter against a standard magnet it was possible to calibrate the second coil to within 1 or 2%. Although there are undoubtedly small variations in winding density between the two coils, we feel that these do not amount to more than a few percent.

Figure 2 shows a typical plot of inverse slopes versus magnetic field strength for various pressures. No effort was made to calibrate the vertical scale since only the horizontal intercept is of interest. It is clear from the figure that the experimental points fall on straight lines and that very little extrapolation is required to obtain the intercepts. A typical set of results is shown in Fig. 3 along with a theoretical curve obtained by fitting Eqs. (26)–(28) to the experimental points as described in Sec. V. The error bars on the experimental points represent the standard deviations of five different runs made over a period of several months.

V. REDUCTION OF THE EXPERIMENTAL RESULTS

As shown in Sec. III, for a $j=1$ to $j=0$ transition the critical axial magnetic field depends only on the three relaxation rates $\gamma_a^{(1)}$, $\gamma_a^{(2)}$, and γ_{ab}. However, each of these rates depends on the partial pressures of the various gases in the laser. In general the rates can be written in the forms

$$\gamma_a^{(2)} = \gamma_a^{(0)} + AP_T, \tag{29}$$

$$\gamma_a^{(1)} = \gamma_a^{(0)} + BP_T, \tag{30}$$

$$\gamma_{ab} = \tfrac{1}{2}(\gamma_a^{(0)} + \gamma_b^{(0)}) + CP_T, \tag{31}$$

where

$$\gamma_a^{(0)} = \gamma_a + DP_T, \quad \gamma_b^{(0)} = \gamma_b + EP_T,$$

$$A = \vec{a}\cdot\vec{P}, \quad B = \vec{b}\cdot\vec{P}, \quad C = \vec{c}\cdot\vec{P}, \quad D = \vec{d}\cdot\vec{P},$$

$$E = \vec{e}\cdot\vec{P}, \quad \vec{P} = \left(\frac{P_{Ne^{20}}}{P_T}, \frac{P_{He^3}}{P_T}, \frac{P_{He^4}}{P_T}\right),$$

where P_T is the total pressure, and $P_{Ne^{20}}$, P_{He^3}, and P_{He^4} are the partial pressures of the gases in the laser.

Equations (29)–(31) contain a total of 17 constants, far more than we can determine from our experimental data, so that we must find ways to eliminate some of the unknown quantities. Fortunately, for the conditions of our experiment, the critical field is very weakly dependent on γ_{ab} ($\partial H_c/\partial\gamma_{ab} \sim 10^{-3}$ G/MHz), thus we can use a very simple approximation for γ_{ab} without affecting our results for $\gamma_a^{(1)}$ and $\gamma_a^{(2)}$. Using the experimental result from Ref. 8 that $\gamma_{ab}/2\pi = 100$ MHz for a total pressure of 2.2 Torr ($P_{He^3}/P_{Ne^{20}} = 10$), and estimating that the radiative linewidth is of the order of 10 MHz we have assumed that

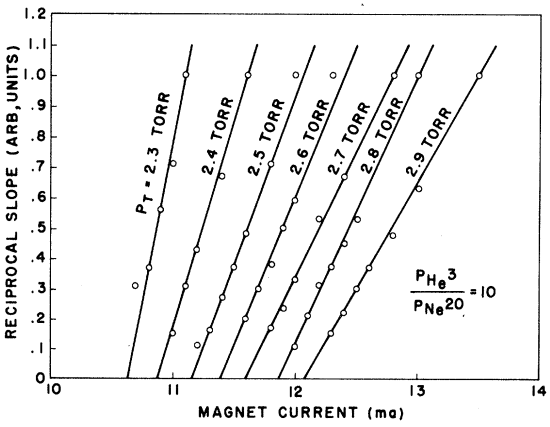

FIG. 2. Experimental values of the reciprocal of the slope of the difference of the intensities of the opposite circular polarizations as a function of cavity detuning, plotted as a function of the current in the magnet coil for various gas pressures. The straight lines are least-squares fits to the experimental points, and intersect the current axis at the current corresponding to the critical axial magnetic field strength.

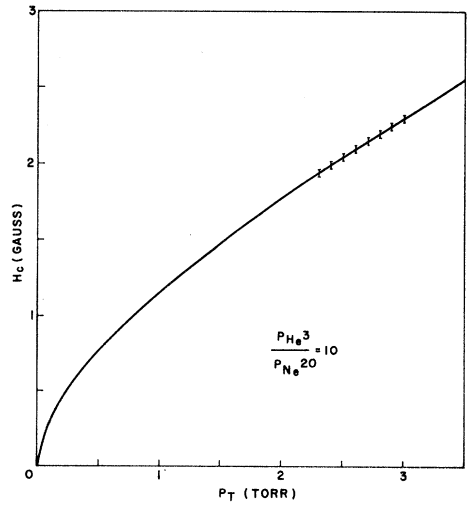

FIG. 3. Critical axial magnetic field strength as a function of total gas pressure for a 10 to 1 mixture of He^3 and Ne^{20}. The solid curve is a plot of Eqs. (26)–(28). The error bars on the experimental points represent the standard deviations of five different runs made over a period of several months.

$\gamma_{ab}/2\pi = [10 + (90/2.2)P_T]$ MHz. This is clearly a rather crude assumption, but more than sufficient for our present purposes. In the preceding paper[9] it was shown that for a $j = 1$ state $\vec{b} = (\frac{5}{3})\vec{a}$ under rather general conditions, thus we replace B in Eq. (30) by $(\frac{5}{3})A$. The experimentally determined cross section[16] for de-excitation of the Ne $2s_2$ state by collisions with He is of the order of 10^{-17} cm^2 which is much smaller than any of the other cross sections, thus we simply set $\vec{d} = (d, 0, 0)$. With these simplifications we can write $\gamma_a^{(1)}$ and $\gamma_a^{(2)}$ as

$$\gamma_a^{(2)} = \gamma_a^{(0)} + AP_T \tag{32}$$

$$\gamma_a^{(1)} = \gamma_a^{(0)} + \tfrac{5}{3} AP_T, \tag{33}$$

$$\text{with } \gamma_a^{(0)} = \gamma_a + dP_{\text{Ne}}. \tag{34}$$

The theoretical calculations in Appendix I give the result $d/\gamma_a = 0.0312$ Torr^{-1}. To show the dependence of the final results on the value chosen for d we have carried out the calculations for the three values $d/\gamma_a = 0$, 0.0312, and 0.312 Torr^{-1}. To obtain a value for γ_a we can make use of the result from Ref. 8 that for a 10 : 1 mixture of He^3 and Ne^{20}, $\gamma_a^{(2)}/2\pi = 20$ MHz at a total pressure of 2.2 Torr. We therefore fitted the critical field data for a 10 : 1 mixture by varying A to minimize the root-mean-square (rms) deviation between the experiment and theory with γ_a determined by the condition $\gamma_a^{(2)}/2\pi = 20$ MHz for $P_T = 2.2$ Torr. The best fit is for $A/2\pi = 1.8$ MHz/Torr which implies $\gamma_a/2\pi = 16$ MHz, or a radiative life time of 10 nsec. An alternate technique is to make use of measurements of γ_{ab} as a function of pressure for the 1.15-μm line[17] ($2s_2 - 2p_4$ transition) which have shown that the extrapolated zero-pressure limit is $\gamma_{ab}/2\pi = 12$ MHz, and the direct measurement of the lifetime of the Ne $2p_4$ state[18] which gave the result $\gamma_b/2\pi = 8.3$ MHz. Combining these results we obtain $\gamma_a/2\pi = 15.7$ MHz ($2s_2$ state), in good agreement with the value given above. To show the dependence of the final results on the value chosen for γ_a we have carried out the calculations for the three values $\gamma_a/2\pi = 14$, 16, and 18 MHz.

We have now reduced the problem to the determination of the three components of the vector $\vec{a}$. For each mixture of gases (defined by the vector $\vec{P}$) we fit the experimental data on critical field as a function of total pressure to determine the value of A for that mixture. From a series of results for different mixtures we then use standard linear regression techniques to solve the equation $A = \vec{a} \cdot \vec{P}$ for the vector $\vec{a}$.

In Table I we list the values for A determined by means of least-squares fits of Eqs. (32)–(34) and (26)–(28) to all the data. The rms deviations between the theoretical and experimental points are between 0.02 and 0.03 G ($\approx 1\%$ of H_c) and are of the order of the scatter of the experimental points about a smooth curve (see Fig. 3). In Table II we list the derived values for the vector, $\vec{a}$, of collision-induced relaxation rates. We found that the values for a_2 and a_3 were essentially independent of the value assumed for d/γ_a. The error limits given in the table are the standard errors of the fit to the data from Table I. Because of the many possible sources of error in the final results it is somewhat difficult to assign realistic error limits. The random errors in the experimental measurements appeared to be less than 1%, but there is a possibility of larger systematic errors in the pressure and magnetic field calibrations. Making a rather subjective estimate of such effects, and our uncertainty concerning the values of γ_a and d, we arrive at the final result

$$\vec{a}/2\pi = (1.5 \pm 1.0,\ 1.85 \pm 0.20,\ 1.52 \pm 0.20) \text{ MHz/Torr}. \tag{35}$$

The large uncertainty in the result for Ne - Ne collisions (a_1) is a reflection of both our uncertainty concerning the true value of d, and the fact Ne was always a minority constituent of the discharge. The rms deviation between all the observed values of H_c and those calculated from $\vec{a}$ as given in Eq. (35) is 0.04 G, or about 2% of H_c.

Defining a vector of cross sections for quadrupole relaxation by $\sigma_i^{(2)} = a_i/(n_i \langle v_i \rangle)$, where n_i is the number density of colliding atoms of the ith type, and $\langle v_i \rangle$ is their mean velocity relative

TABLE I. Experimental results for A for various gas mixtures.

$\frac{P_{He}}{P_{Ne^{20}}}$	$\frac{P_{He^3}}{P_{He}}$	$\vec{P}$	$A/2\pi$ (MHz/Torr) $d/\gamma_a = 0$ $\gamma_a/2\pi$ = (MHz) 14	16	18	$d/\gamma_a = 0.0312$ (Torr^{-1}) $\gamma_a/2\pi$ = (MHz) 14	16	18	$d/\gamma_a = 0.312$ (Torr^{-1}) $\gamma_a/2\pi$ = (MHz) 14	16	18
10	1	(0.091, 0.909, 0.000)	1.938	1.797	1.674	1.930	1.789	1.666	1.861	1.720	1.598
10	0.75	(0.091, 0.682, 0.227)	1.866	1.731	1.614	1.857	1.723	1.606	1.787	1.653	1.536
10	0.60	(0.091, 0.545, 0.364)	1.893	1.759	1.641	1.885	1.751	1.632	1.812	1.678	1.561
10	0.25	(0.091, 0.227, 0.682)	1.709	1.593	1.489	1.700	1.583	1.480	1.623	1.505	1.402
7.5	1	(0.117, 0.883, 0.000)	2.046	1.892	1.763	2.030	1.882	1.753	1.941	1.794	1.667
5	1	(0.167, 0.833, 0.000)	1.929	1.789	1.666	1.914	1.774	1.652	1.790	1.651	1.531

TABLE II. Experimental results for the relaxation-rate vector $\vec{a}$.

$\gamma_a/2\pi$ (MHz)	d/γ_a (Torr^{-1})	$\vec{a}/2\pi$ (MHz/Torr) a_1	a_2	a_3
	0	1.7 ± 0.8		
14	0.0312	1.6 ± 0.8	2.00 ± 0.10	1.63 ± 0.10
	0.312	0.9 ± 0.8		
	0	1.6 ± 0.7		
16	0.0312	1.5 ± 0.7	1.85 ± 0.10	1.52 ± 0.09
	0.312	0.8 ± 0.7		
	0	1.5 ± 0.7		
18	0.0312	1.4 ± 0.7	1.72 ± 0.09	1.42 ± 0.08
	0.312	0.7 ± 0.7		

to the Ne^{20} atoms, and assuming a gas temperature of 500°K, we obtain the result

$$\vec{\sigma}^{(2)}(\text{experiment})$$

$$= (5 \pm 3,\ 2.99 \pm 0.32,\ 2.78 \pm 0.37) \times 10^{-15}\ \text{cm}^2. \quad (36)$$

The components of this vector are then the cross sections for the collision-induced relaxation of the electric quadrupole moment of the Ne^{20} $2s_2$ state as a result of collisions with ground-state Ne^{20}, He^3, and He^4 atoms respectively. The corresponding cross sections for the magnetic dipole moment are simply $\frac{5}{3}$ times those for the quadrupole moment. Note that these cross sections are only for collisions in which the electronic excitation is not transferred to the colliding atom, or what we have defined as m_j-mixing collisions.

Decomps and Dumont have recently reported measurements of the relaxation of the Ne $2s_2$ state by means of a Hanle effect experiment with laser excitation.[19] Their results are $\sigma_{Ne}^{(2)} = (9.5 \pm 2.0) \times 10^{-15}$ cm^2, $\sigma_{He}^{(2)} = (1.7 \pm 0.7) \times 10^{-15}$ cm^2, $\gamma_a/2\pi = (18.7 \pm 2.0)$ MHz, and $d/\gamma_a = 0.008$ Torr^{-1}. (They do not specify what isotopes were used in their experiment.) The error limits on these results overlap those on our results, although we would have expected somewhat closer agreement. However, the He cross sections are in better agreement if we use their values for γ_a and d/γ_a (see Table II).

VI. COMPARISON WITH THEORETICAL RESULTS

We now compare the experimental cross sections with theoretical values for the cross sections for van der Waals collisions using the theoretical expressions obtained in the preceding paper.[9] In the Appendix we show that the m_j-mixing cross sections for resonant collisions between a Ne atom in the $2s_2$ state and one in the ground state are an order of magnitude smaller than either the experimental values or the theoretical values for van der Waals or nonresonant collisions, thus we will neglect resonant collisions in the following.

As given in Eq. (47) of Ref. 9, if we assume that the motion of the colliding atoms follows a linear classical path, the m_j-mixing cross sections $\sigma_j^{(\chi)}(i)$ for an atom in a state of angular momentum j colliding with the ith perturbing atom are

$$\sigma_j^{(\chi)}(i) = D_i (\langle v_i^{3/5} \rangle / \langle v_i \rangle)\, \phi_j^{(\chi)}, \quad (37)$$

where

$$D_i = (\pi p^2 p^2 i / 16\hbar \langle \Delta E_i \rangle)^{2/5},$$

and $\phi_j^{(\chi)}$ is a geometric factor which is tabulated in Table I of Ref. 9. For $j = 1$, $\phi_1^{(1)} = 4.062$, and $\phi_1^{(2)} = 2.437$. If we assume a Maxwellian distribution for the relative velocity, we then have

$$\langle v_i^{3/5} \rangle = 2\Gamma(\tfrac{9}{5})\, \pi^{-1/2} (2kT/\mu_i)^{3/10}, \quad (38a)$$

and

$$\langle v_i \rangle = (8kT/\pi\mu_i)^{1/2}, \quad (38b)$$

where μ_i is the reduced mass for the colliding pair of atoms, k is the Boltzmann constant, and T is the temperature of the medium, which is taken as 500°K in our experiment.

As for calculating p^2 and p_i^2, we use the Slater radial wave function[20] given by

$$\psi(r) = r^{(n_i^* - 1)} \exp\{-Z_i^* r/n_i^*\}. \quad (39)$$

The basis for this wave function is the fact that an electron in an atom does not "feel" the presence of the nucleus completely, inasmuch as the electron is screened from the nucleus by the other electrons. Hence an electron in the atom moves as though in a field of effective nuclear charge $Z_i^* e$. At large distances, this wave function behaves like a hydrogenlike wave function of the effective principal quantum number n^*. It is easy to show that

$$p_i^2 = e^2 a_0^2 (n_i^* + 1)(n_i^* + \tfrac{1}{2}) n_i^{*2} / Z_i^{*2} \quad (40)$$

and a similar expression applies to p^2. The effective principal quantum number n^* and the effective nuclear charge Z^* can be found from the Slater rule.[20] For He in the ground state, $n^* = 1$ and $Z^* = 1.70$. For Ne in the ground state $n^* = 2$ and $Z^* = 5.85$. For Ne in the $2s_2$ state, $n^* = 3.7$ and $Z^* = 1$. On the basis of these parameters, we obtain 1742 D^2 for p^2, and 6.69 and 5.65 D^2 for the p_i^2 of He and Ne, respectively.

Finally, we need values for $\langle \Delta E_i \rangle$ for the com-

plete determination of the cross sections. From the definition of $\langle \Delta E_i \rangle$ given in Ref. 9, for an accurate determination, one requires information about oscillator strengths of the states involved during the collision. The oscillator strengths of various low-lying states of atoms significant in gas lasers have been measured by Bennett and co-workers,[18] but they are not sufficient to estimate an accurate value of $\langle \Delta E_i \rangle$. As far as the Ne-He collision is concerned, the excursions from the ground state to the 2^1P state of He (simultaneously the Ne making a transit from the $2s_2$ state to the ground state) are expected to give a large contribution to the dispersion potential; however, other states such as 3^1S, 3^1P, etc., of He, and $2p$, $3s$, etc., of Ne will also give significant contributions. A similar complication applies to the Ne-Ne collision. A more appropriate way to determine $\langle \Delta E_i \rangle$ is through experiment if one is sure the van der Waals collision describes the collision process correctly. However, the cross sections are proportional to $\langle \Delta E_i \rangle^{-2/5}$, thus a small uncertainty cannot significantly affect the values for the cross sections. Since the $2s_2$ state of the Ne atom is optically connected to the levels immediately above and below it, as an approximation we set $\langle \Delta E_i \rangle$ equal to 1.98×10^5 cm^{-1} (the first ionization potential of He) and 1.74×10^5 cm^{-1} (the first ionization potential of Ne), respectively. This approximation was also used by Hansch *et al.*[21]

On the basis of the above atomic parameters, we calculated the cross sections for the quadrupole relaxation of the Ne^{20} $2s_2$ state as a result of collisions with ground-state Ne^{20}, He^3, and He^4 atoms. The result, in the same notation as Eq. (36), is

$$\vec{\sigma}^{(2)}\ (\text{theory}) = (7.75,\ 5.76,\ 6.00)\times10^{-15}\ \text{cm}^2. \quad (41)$$

The result for Ne-Ne collisions, $\sigma_1^{(2)}$ falls within the error brackets on the experimental result given in Eq. (36); the Ne-He cross sections, $\sigma_2^{(2)}$ and $\sigma_3^{(2)}$, are about a factor of 2 larger than the corresponding experimental results in Eq. (36). However, in view of the many approximations introduced in the calculation of the absolute cross sections, a discrepancy of this order is not surprising. For example, one sees from Eq. (40) that the quantity p^2 (or p_i^2) is a strong function of the effective charge Z, and therefore the cross section varies with the effective change as $(ZZ_i)^{4/5}$. An error in the assignment of the effective charge would result in a corresponding error in the cross section. An accurate cross section can be calculated only when one has accurate numbers for p^2, p_i^2, and $\langle \Delta E_1 \rangle$. Nevertheless, the results strongly suggest that van der Waals collisions are responsible for the observed effects.

ACKNOWLEDGMENTS

We wish to thank J. P. Gordon for many stimulating discussions and suggestions. We also wish to acknowledge helpful discussions with W. E. Lamb, Jr., and W. R. Bennett, Jr.

APPENDIX

Calculation of the Cross Sections for Resonant Collisions

As given by Eq. (19) of the proceeding paper,[9] the multipole moment relaxation cross sections should obey the sum rule

$$\sum_{\chi=0}^{2j} (-1)^{\chi}(2\chi+1)\sigma_j^{(\chi)}(b_i v_i) = (2j+1)\sigma_j^{(0)}(b_i v_i). \quad (A1)$$

For the Ne $2s_2$ state (a $j=1$ state), Eq. (A1) becomes

$$5\sigma_1^{(2)}(b_i v_i) - 3\sigma_1^{(1)}(b_i v_i) = 2\sigma_1^{(0)}(b_i v_i). \quad (A2)$$

It was shown by Omont[13] that for resonant collisions $\sigma_1^{(1)}(b_i v_i)$ and $\sigma_1^{(2)}(b_i v_i)$ are given by

$$\sigma_1^{(1)}(b_i v_i) = \tfrac{8}{3}\left\{\sin^2\frac{A}{b_i^2} - \tfrac{1}{2}\sin^4\frac{A}{b_i^2}\right\}, \quad (A3)$$

$$\sigma_1^{(2)}(b_i v_i) = \tfrac{8}{3}\left\{\sin^2\frac{A}{b_i^2} - \tfrac{7}{10}\sin^4\frac{A}{b_i^2}\right\}, \quad (A4)$$

where

$$A = |\langle 0||p||1\rangle|^2/3\hbar v_i .$$

The results in Eqs. (A3) and (A4) can also be readily obtained by the method described in the preceding paper.[9]

Substituting Eqs. (A3) and (A4) into (A2), we obtain the cross section for the population relaxation as

$$\sigma_1^{(0)}(b_i v_i) = \tfrac{8}{3}\left\{\sin^2\frac{A}{b_i^2} - \sin^4\frac{A}{b_i^2}\right\}. \quad (A5)$$

Integrating over the impact parameter and also averaging over the relative velocity, we obtain the total cross sections as

$$\sigma_1^{(0)} = (\lambda^3/48\pi\langle v_i\rangle)\Gamma,$$

$$\sigma_1^{(1)} = (3\lambda^3/96\pi\langle v_i\rangle)\Gamma, \quad (A6)$$

$$\sigma_1^{(2)} = (13\lambda^3/480\pi\langle v_i\rangle)\Gamma ,$$

where Γ is the rate of the (electric dipole) transition of the atom in the excited state to the ground state and is given by $\Gamma = 32\pi^3|\langle 1||p||0\rangle|^2/3\lambda^3$. The quantity λ is the wavelength for this transition. For the Ne $2s_2$ state, Γ is essentially identical to γ_a (within about 10%, because of branching to other states) described in the text, and $\gamma_a/2\pi$ is given a value of 16 MHz. The wavelength corresponding to the transition from Ne $2s_2$ state to the ground state is 625 Å. The relative velocity of Ne atoms at 500°K is 1.025×10^5 cm/sec. The substitution of these values for Γ, λ, and $\langle v_i\rangle$ into Eq. (A6) gives

$$\sigma_1^{(0)} = 1.60\times10^{-15}\ \text{cm}^2 ,$$

$$\sigma_1^{(1)} = 2.40\times10^{-15}\ \text{cm}^2 , \qquad \text{(A7)}$$

$$\sigma_1^{(2)} = 2.08\times10^{-15}\ \text{cm}^2 .$$

The contributions to the σ due to m_j - mixing collision are thus

$$\Lambda_1^{(1)} = 0.80\times10^{-15}\ \text{cm}^2 ,$$

$$\text{(A8)}$$

$$\Lambda_1^{(2)} = 0.48\times10^{-15}\ \text{cm}^2 .$$

Comparing these cross sections with those for van der Waals or nonresonant collisions calculated in Sec. VI we find that the resonant cross sections are about an order of magnitude smaller than the nonresonant cross sections. They are also about an order of magnitude smaller than the experimental results given in Sec. V. Therefore, we can neglect the effects of resonant collisions in the calculation of the m_j - mixing collision cross sections.

Since the nonresonant collisions do not contribute to the decay of the population of the excited state, the most significant contribution to the monopole cross section is the resonant collision term. From the cross section given in Eq. (A7) we obtain the result $d/\gamma_a = 0.0312\ \text{Torr}^{-1}$ which is used in Sec. V. This value is of the same order as that measured by Decomps and Dumont.[19] If we interpret the "hard-collision" cross section reported in Ref. 17 as including resonant collisions as well as other effects, we can obtain an upper limit on d/γ_a of about $0.3\ \text{Torr}^{-1}$.

As pointed out by D'yakonov and Perel'[11] in order for the above calculation to be meaningful, the cross sections given in Eq. (A6) should be small compared with the square of the mean distance between atoms, which leads to the condition $n\lambda^3(\Gamma/\Delta\omega)^{3/2} \ll 1$, where $\Delta\omega$ is the Doppler width for the resonant transition. For a pressure of 1 Torr (somewhat higher than used in our experiments) the left-hand side of the above inequality has a value of about 3×10^{-4}, thus the condition is well satisfied.

---

*Permanent address: Department of Electrical Engineering, Duke University, Durham, N. C.

[1]W. E. Lamb, Jr., Phys. Rev. 134, A1429 (1964).

[2]M. Sargent, III, W. E. Lamb, Jr., and R. L. Fork, Phys. Rev. 164, 436, 450 (1967).

[3]R. L. Fork and M. A. Pollack, Phys. Rev. 139, A1408 (1965).

[4]W. J. Tomlinson and R. L. Fork, Phys. Rev. 164, 466 (1967).

[5]R. L. Fork, W. J. Tomlinson, and L. J. Heilos, Appl. Phys. Letters 8, 162 (1966).

[6]H. de Lang and G. Bouwhuis, Phys. Letters 20, 383 (1966).

[7]Similar effects have also been observed in a He-Xe laser, but since it is not possible at the present time to obtain pure Xe isotopes the interpretation of the experiments is more difficult than for the He-Ne laser.

[8]W. J. Tomlinson and R. L. Fork, Phys. Rev. Letters 20, 647 (1968).

[9]C. H. Wang and W. J. Tomlinson, preceding paper, Phys. Rev. 181, (1969).

[10]W. Happer and E. B. Saloman, Phys. Rev. 160, 23 (1967).

[11]M. I. D'yakonov and V. I. Perel', Zh. Eksperim. i Teor. Fiz. 47, 1483 (1964) [English transl.: Soviet Phys. – JETP 20, 997 (1965)]; M. I. D'yakonov and V. I. Perel', Zh. Eksperim. i Teor. Fiz. 48, 345 (1965) [English transl.: Soviet Phys. – JETP 21, 227 (1965)].

[12]M. I. D'yakonov and V. I. Perel', Opt. i Spektroskopia 20, 472 (1966) [English transl.: Opt. Spectroy. 20, 257 (1966)].

[13]A. Omont, J. Phys. (Paris) 26, 26 (1965).

[14]A. R. Edmonds, Angular Momentum in Quantum Mechanics (Princeton University Press, Princeton, New Jersey, 1960).

[15]W. J. Tomlinson and R. L. Fork, Appl. Opt. 8, 121 (1969).

[16]A. Javan, W. R. Bennett, and D. R. Herriott, Phys. Rev. Letters 6, 106 (1961).

[17]A. Szöke and A. Javan, Phys. Rev. 145, 137 (1966).

[18]W. R. Bennett, Jr., and P. J. Kindlmann, Phys. Rev. 149, 38 (1966).

[19]B. Decomps and M. Dumont, IEEE J. Quantum Electron. QE-4, 916 (1969).

[20]J. C. Slater, Phys. Rev. 36, 57 (1930).

[21]T. Hansch, R. Odenwald, and P. Toschek, Z. Physik 209, 478 (1968).